## **BPB Reports**

#### Report

# Modification of the MSD-AFLP Method for Detection of 5-Hydroxymethylcytosine and Its Application to NGS

Toshiki Aiba, <sup>a,b,\*</sup> Akiko Hayashi, <sup>b</sup> Shinji Sato, <sup>c</sup> Sumitaka Hasegawa, <sup>a</sup> Harunobu Yunokawa, <sup>c</sup> Tsuruoka Chizuru, <sup>b</sup> Tatsuhiko Imaoka, <sup>b</sup> and Toshiyuki Saito <sup>b</sup>

<sup>a</sup>Department of Charged Particle Therapy Research, QST Hospital, National Institutes for Quantum Science and Technology, 4-9-1 Anagawa, Inage-ku, Chiba 263-8555, Japan; <sup>b</sup>Department of Radiation Effects Research, Institute for Radiological Science, National Institutes for Quantum Science and Technology, Chiba 263-8555, Japan; <sup>c</sup>Maze, Inc., Tokyo 193-0835, Japan

Received August 1, 2025; Accepted October 24, 2025

5-Hydroxymethylcytosine (5hmC) is beginning to be expected to play a role as a diagnostic and prognostic marker of diseases. On the other hand, we developed the methylated-site display-amplified fragment length polymorphism (MSD-AFLP), an affordable, large-scale (approximately 40,000-50,000 CpG sites), highly sensitive methylation profiling method, and applied it to environmental health and disease biomarker discovery research. Herein, we attempted to modify the MSD-AFLP method to detect 5hmC. To validate this method, we compared hydroxymethylation levels among tissues using mouse samples to determine whether this method could detect tissue-specific differential 5hmC. We also considered combining this method with next generation sequencing (NGS). Comparisons using AFLP revealed that in some sites, the variation in hydroxymethylated DNA was greater than that in methylated DNA between tissues. Therefore, we determined the hydroxymethylation levels at these sites using Glucosylation-mediated restriction enzyme sensitive qPCR (gRES-qPCR) to confirm the accuracy of the AFLP analysis. The differences in hydroxymethylation levels between tissues were similar between the two methods. The protocol for combination with NGS was evaluated by comparing the AFLP data with 11 DNA fragments. The differences in hydroxymethylation levels between tissues were similar between the two methods. Cluster analysis demonstrated that NGS data were comparable to AFLP data in detecting differential and contrasting hydroxymethylation patterns across tissues. This method, based on the MSD-AFLP technique, will contribute to various epigenetics-based research, including the discovery of biomarkers and therapeutic drug targets.

**Key words** 5-hydroxymethylcytosine, methylated-site display-amplified fragment length polymorphism, next-generation sequencing

### INTRODUCTION

DNA methylation is involved in the regulation of gene expression during development and differentiation, and has attracted attention in regenerative medicine using induced pluripotent stem (iPS) cells for cell reprogramming via DNA methylation changes.<sup>1)</sup> It is also related to human diseases including cancer, and it has been suggested that DNA methylation could be a target for prevention, biomarkers, and treatment.<sup>2)</sup> In particular, the mechanism behind the "Developmental Origins of Health and Disease (DOHaD) hypothesis" suggests that epigenetic changes, such as DNA methylation, caused by fetal exposure to environmental factors, including environmental chemicals, may alter disease susceptibility, and these may function as biomarkers.<sup>3)</sup> Therefore, several methods to detect genome-wide 5-methylcytosine (5mC) have

been developed combining methylation arrays and sequencing, etc., with antibody- or binding-protein-mediated enrichment, bisulfite conversion, enzymatic modification, and single-molecule approaches.<sup>4)</sup>

Recently, we have developed a convenient, large-scale, and highly sensitive methylation-profiling method, methylated-site display-amplified fragment length polymorphism (MSD-AFLP), to detect these changes. MSD-AFLP is a method based on a unique technique for the preparation of DNA libraries using methylation sensitive restriction enzyme and combining it with AFLP analysis. This method is advantageous in its convenience and cost-effectiveness to detect abnormal epigenetic alterations in DNA methylation in experiments where multiple samples are processed simultaneously. We applied this method to study the effects of environmental chemicals on the fetal epigenome and explored disease-specific methylated

<sup>\*</sup>To whom correspondence should be addressed. e-mail: aiba.toshiki@qst.go.jp



CpGs in human male reproductive disorders.<sup>6,7)</sup>

DNA methylation is actively demethylated by converting it to 5-hydroxymethylcytosine (5hmC) via Ten-eleven Translocation (TET) protein.8) In contrast, many reports have shown that 5hmC functions as an intermediate in demethylation, is a stable chemical modification in the genome involved in gene expression control and cell differentiation, and is expected to play a role as a diagnostic and prognostic marker for diseases.<sup>9)</sup> Consequently, technologies enabling the separate detection of 5mC and 5hmC - which were previously indistinguishable using methods including MSD-AFLP - have been developed, and existing methods for detecting methylated DNA have been modified. 10-13) Therefore, we investigated the possibility of modifying the MSD-AFLP method, a recently developed affordable, large-scale, and highly sensitive methylation profiling method, into the hMSD-AFLP method, a profiling method for comprehensively and sensitively detecting hydroxymethylated DNA. In the MSD-AFLP method, it is possible to predict the genomic location of DNA fragments corresponding to AFLP peaks using the Genome DNA Fragment Database (GFDB) based on indirect information such as restriction enzyme selection, selective nucleotides (NN1 and NN2), and fragment length range (size). Many of the fragments (85.4%) in AFLP chart do not overlap in size and are predicted to display a single peak, and therefore, their genomic positions can be predicted using only GFDB.5)

The development of next-generation sequencing (NGS) has been remarkable, and it has been combined with methylation and hydroxymethylation analyses.<sup>14,15)</sup> Therefore, we combined the hMSD-AFLP method with NGS to directly identify variable genes at genomic locations instead of predicting them by

GFDB for more accurate and smoother identification.

#### MATERIALS AND METHODS

**Reagents** The reagents and materials used in this study were purchased from the manufacturers indicated in parentheses: T4 DNA ligase, and restriction enzymes MspI, SbfI, and EpiMark 5-mC and 5-hmC Analysis Kit including T4-βglucosyltransferase and UDP-glucose (New England Biolabs, MA, USA); oligonucleotides (Eurofins Scientific SE, Luxembourg, Luxembourg); magnetic beads coated with streptavidin (Dynabeads M-280 Streptavidin) (Dynal, Oslo, Norway); TITANIUM Tag DNA polymerase and TB Green Premix Ex Tag II (Tli RNaseH Plus) (Takara Bio, Kusatsu, Japan); POP-7 Polymer, GeneScan 500 LIZ Size Standard, Qubit dsDNA HS Assay Kit (ThermoFisher Scientific, San Diego, CA, USA); NucleoMag NGS Clean-up and Size Select (Macherey-Nagel, Duren, Germany); xGen Stubby Adapter and UDI Primer Pairs, Index 1-16 (Integrated DNA Technologies, Coralville, IA, USA).

**Mouse Genomic DNA** Mouse genomic DNA was obtained in a previous study.<sup>5)</sup> Briefly, mouse genomic DNA from the liver and kidney was originally obtained from thirteen-week-old male C57BL/6J mice (n = 3) and purified using the AllPrep DNA/RNA Mini Kit for MSD-AFLP.

hMSD-AFLP A flowchart of the hMSD library preparation steps is shown in Fig. 1. The MSD-AFLP protocol was modified to detect 5hmC. First, genomic DNA (200 ng) digested with a methylation-insensitive eight-base cutter Sbfl was ligated with a biotinylated adaptor (Adaptor A) (5'-(Biotin) TCCGACTGGTATCAACGCAGAGTACTA

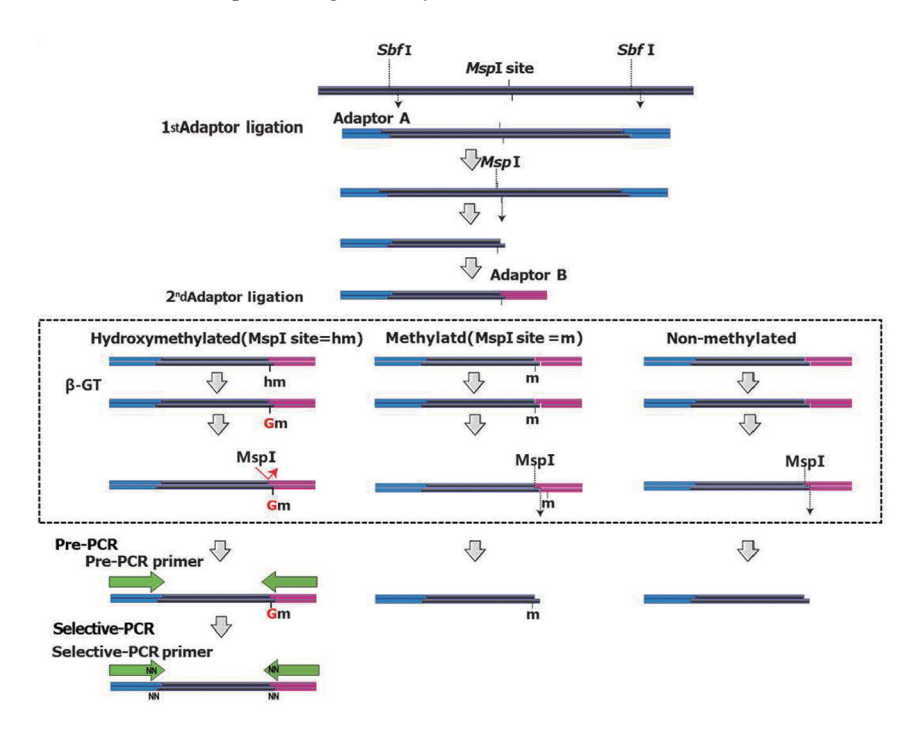


Fig. 1. Flowchart of hMSD Library Preparation

Genomic DNA (200 ng) was digested with 10 units of the primary restriction enzyme SbfI for 1 h and then ligated with 0.5 nmol Adaptor A (blue) using 400 units of T4 DNA ligase for 30 min. The treated sample was then digested with 100 units of the methylation-insensitive restriction enzyme MspI followed by ligation of the ends of the DNA fragment with Adaptor B (red) on MspI site. Up to this point, the procedures are the same as the first half of the MSD-library preparation steps. The ligated DNA fragments were then instead of HpaII digestion in the MSD library,  $\beta$ -glucosylated with T4- $\beta$ -glucosylaterase (10 units) for 12 h and digested with Msp I (100 units) for 1 h. As a result of  $\beta$ -glucosylation of the hydroxylmethyl group, DNA fragments with a hydroxymethyl CpG are protected from MspI digestion (red arrow) and retain Adaptor B, whereas all other fragments lose this adaptor (box in broken line); this step is a modification for detecting 5hmC. The DNA fragments were then subjected to pre-PCR using specific primers for Adaptors A and B. Fragments that did not contain Adaptor B at this stage were not amplified. Subpopulations of the pre-PCR amplicons (hMSD library) were then amplified by selective-PCR using 6-carboxyfluorescein (6-FAM)-labeled selective-PCR primers. Finally, the selective-PCR products were electrophoresed using a capillary sequencer and separated by length.

GAGTTGCA-3', 5'-pACTCTAGTACTCTGCGTTGATAC-CAGTCGGA-3') using 400 units of T4 DNA ligase. Next, the ligated products were digested with 100 units of CCGG cutter MspI for 1 h. The resulting DNA fragments were captured using Dynabeads M-280 Streptavidin and washed with washing buffer (10 mM Tris HCl, 1 mM EDTA, 2 M NaCl, pH7.5) and TE (1 mM Tris HCl, 0.1 mM EDTA, pH 7.5) three times. The DNA fragments were then ligated with Adaptor B (5' -AATGGCTACACGAACTCGGTTCATGACC-3', 5'-CGG GTCATGAACCGAGTTCGTGTAGCCATT-3'). Up to this point, the procedure was the same as in the first half of the MSD-library preparation steps. After another washing in the same manner, the products were β-glucosidated with T4-β-glucosyltransferase and UDP-glucose and digested with MspI on magnetic beads. While remaining on the beads, the MspI-digested DNA fragments were then amplified with pre-PCR primers (5'-AATGGCTACACGAACTCGGTTCAT-GACACGG-3', 5'-TCCGAC TGGTATCAACGCAGA-3') under the same conditions for MSD library preparation, which is 25 cycles of denaturation at 95°C for 20 s, annealing at 58°C for 20 s, and extension at 72°C for 90 s. The resulting solution containing the hMSD library was used as a template for selective-PCR. The selective-PCR step was based on the MSD-AFLP using different primer pairs (5'-(FAM)AATGGC-TACACGAACTCGGTTCATGACAII INN-3', 5' -AGAG-TACTAGAGTTGCAGGNN-3').5) Of the 256 possible PCR sets, eight selective primer sets were used, including five that suggested the all 11 DNA fragments described in our previous study.5) The products of selective-PCR were electrophoresed using a capillary sequencer to obtain an AFLP chart. Data analysis was performed using GeneMapper ID Software v3.7 (Thermo Fisher Scientific) and HiAL version 5.2 software (Maze, Tokyo, Japan) as previously described.<sup>5)</sup>

Glucosylation-Mediated Restriction Enzyme Sensitive qPCR (gRES-qPCR) The EpiMark kit (NEB) was used to quantify the relative levels of 5hmC at selected loci in the mouse kidney and liver DNA. Briefly, purified genomic DNA (200 ng) was divided into two part, treated with T4-β-glucosyltransferase and either digested with or without MspI for a further 12–16 h at 37°C. The two resulting digested DNA samples were subjected to relative quantitative PCR measurements using Mx3000P (Agilent) with locus-specific primers for previously reported peak ID 26 (5'-ACCAGC-TACACGGCT CGTAAT-3', 5'-TAAAACGGGTGGAAGGA-GATT-3') and ID 59 (5'-TTTTGGGAA CTTGAACCAGTG, 5'-TCTTCTGGAAGGTTTGCTGTG-3'). The protocol was based on our Methylation restriction enzyme-based (MSRE)-PCR.

Library preparation for NGS The resulting amplicons (hMSD library) were amplified by selective-PCR using five different primer pairs (5'-(FAM) or 5'-AATGGCTACAC-GAACTCGGTTCATGAC AIIINN-3', NN = TT, TA, TA, TA, or CA; reverse, 5'-AGAGTACTAGAGTTGCAGGNN-3', NN = GC, GC, AA, AG, or AG) representing 11 DNA fragments, as previously described. The selective-PCR products were purified to approximately 200-1000 bp using Nucleo-Mag NGS Clean-up and Size Select using the 0.6X–2.0X size selection. The purified product was quantified using the Qubit dsDNA HS Assay Kit (Thermo Fisher Scientific). The 250 ng product was ligated using 1600 units T4 DNA ligase and incubation for 15 min at 20°C with xGen Stubby Adapter diluted 1:100 (final concentration). Next, a post-ligation cleanup was

performed with NucleoMag NGS Clean-up and 0.55X–0.85X size selection. We added UDI Primer Pairs for index sequences at PCR using TITANIUM Taq DNA polymerase to maintain sample traceability through sequencing under the following conditions: 12 cycles of denaturation at 95°C for 30 s, annealing at 60°C for 30 s, and extension at 72°C for 30 s. The products were purified using NucleoMag NGS Clean-up and Size Select using the 0.55X–0.85X size selection. Finally, the purified products were cleaned with NucleoMag NGS Clean-up and Size Select with 0.9X size selection. Final libraries were checked for quality using Qubit (Thermo Fisher Scientific) and GenNext NGS Library Quantification Kit using Mx3000P (Agilent). After library preparation, paired-end sequencing (PE150) was performed using the Illumina NovaSeq X Plus platform at Novogene Co., Ltd. (Beijing, China)

**Data Analysis** FASTQ files were analyzed using the CLC Genomics Workbench 24 (Qiagen, Hilden, Germany). Sequences were trimmed the hMSD-AFLP adaptor, aligned to the mouse genome assembly MGSCv37 (mm9), and TPM calculated according to the BED file (Supp. S1) created using DNA fragment location information from GFDB.

**Statistical Analyses** Differences in hydroxymethylation levels between groups were analyzed by Student's t-test using Microsoft Excel 365 (Microsoft, USA).

#### **RESULTS**

Conceptual Design of hMSD-AFLP and Its Accuracy for Hydroxymethylated CpG As shown in Fig. 1, adapters A and B were ligated to the genomic DNA in the same manner as in the MSD library, and the DNA sample was digested with MspI after β-glucosylation instead of HpaII digestion (a methylation-sensitive isoschizomer used in MSD-AFLP). In this step, if the adapter B-ligated fragment did not contain a hydroxymethylated CpG, adapter B was removed, and only the DNA fragments that retained adapter B were amplified by the subsequent pre-PCR to generate the hMSD library. Therefore, it was amplified only if the nearest MspI-CpG, which was closest to the primary restriction enzyme (SfbI) site was hydroxymethylated. The pre-PCR amplicons (hMSD library) were then amplified as subpopulations by selective PCR using 6-carboxyfluorescein (6-FAM)-labeled selective PCR primers. Finally, the selective PCR products were electrophoresed in a capillary sequencer and separated by length.

Using the modified MSD-AFLP method for detecting hydroxymethylation (hMSD-AFLP method), we compared the hydroxymethylation levels in two mouse tissues (liver and kidney). For each tissue, eight selective primer sets were used, including five primer sets representing all 11 DNA fragments reported previously from 256 possible PCR sets as previously descibed.<sup>5)</sup> We detected 1,400 AFLP signals and succeeded in identifying CpG sites with different hydroxymethylation levels between the tissues (Fig. 2). Next, we focused on the 11 DNA fragments from our previous study<sup>5)</sup> and compared hydroxymethylated (5hmC) and methylated (5mC+5hmC) DNA between tissues. Most showed similar tendencies. However, we found that there were some sites where the fluctuation rate of hydroxymethylated DNA was greater than that of methylated DNA (Fig. 3A; see Fig. 4b of Ref. 5) for methylation). Therefore, we used the conventional gRES-qPCR method to confirm the hydroxymethylation levels of two sites (ID 26,59), where hMSD-AFLP suggested substantial differences

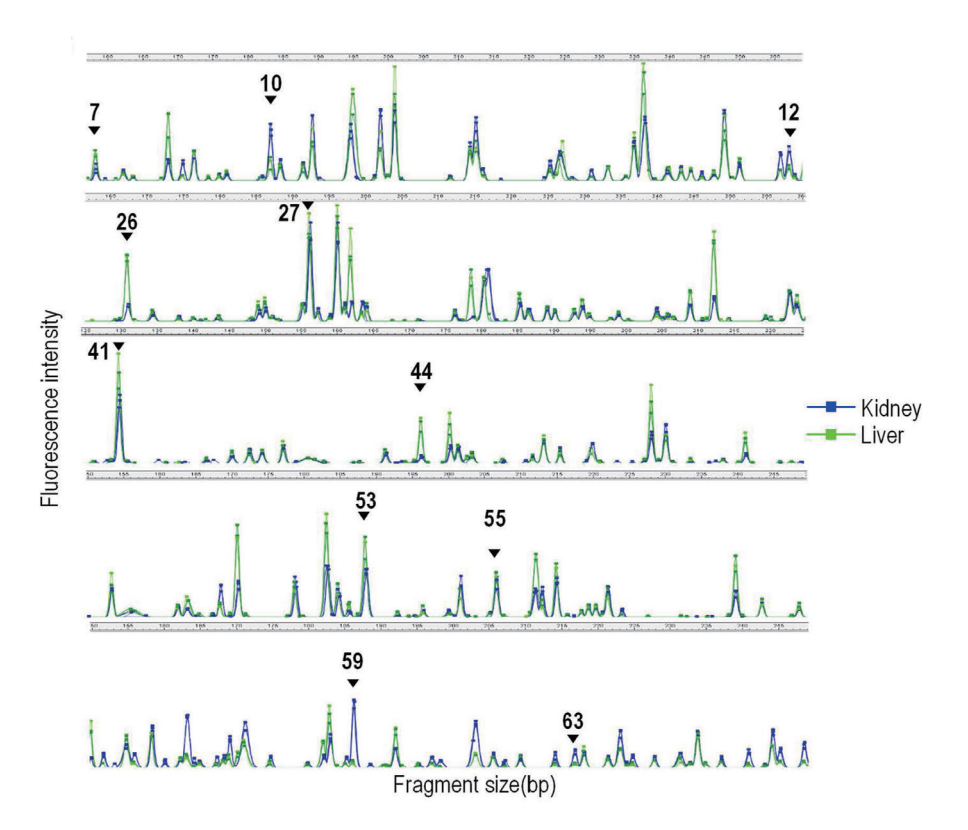


Fig. 2. AFLP Electropherogram Peak Charts Obtained by hMSD Analysis

Each color electropherogram represents data from the kidney; (blue) green or liver (green). Six electropherograms are shown in the charts (three from each tissue). Black numbers and arrows indicate peak IDs (11 CpGs) analyzed with MSD-AFLP and MSRE-PCR 5). Several CpGs were detected as differentially hydroxymethylated among tissue, as seen in peaks 26, 44, and 59, with good consistency among the three samples.

in hydroxymethylation between tissues and whose rate of variation was greater than the change in methylation level. Both fragments showed values similar to those of gRES-qPCR, suggesting that they were nearly identical (Fig. 3A, B). Furthermore, the scatter plot of the relative values of the two methods showed a strong correlation ( $R^2 = 0.9655$ ) (Fig. 3C).

Application of hMSD Libraries to NGS We examined the reproducibility of NGS by comparing two NGS libraries independently constructed from the hMSD library of kidney DNA. Of the eight primer sets used for AFLP and analysis, five selective primer sets representing 11 DNA fragments from our previous study5) were used to perform NGS analysis at 1 Gb/8 samples for each library, resulting in a comparison of a total of 15,664 types of reads (of which 895 contained the selective bases of the primers used). The coefficient of determination, R2, was 0.907 between replicates without 6-FAM and 0.895 between replicates with and without 6-FAM, indicating a reliable reproducibility of NGS (Fig. 4). Next, we compared the AFLP and NGS data and found that all 11 regions were similar, and seven out of eight regions (87.5%) detected as tissue-specific differentially 5hmC candidates by AFLP were also detected by NGS, suggesting that they were consistent with each other (Fig. 5A, B). Furthermore, a scatter plot of the relative values of the two methods indicated a strong correlation ( $R^2 = 0.9097$ ) (Fig. 5C).

#### DISCUSSION

Although the MSD-AFLP method covers only about 0.2% (0.22% in mouse and 0.15% in human) of the CpG sites in

the genome, it is relatively low-cost compared with NGSbased genome-wide DNA methylation analysis. It provides CpG methylation level profiles of a large number of CpGs (approximately 40,000-50,000) in a single analysis with almost the same accuracy as MSRE-PCR analysis.5) Therefore, in this study, we first modified the MSD-AFLP method to enable hydroxymethylation analysis. 5hmC has tissue-specific distribution that coincides with gene body methylation.<sup>16)</sup> Although a high proportion of 5-hmC has been reported in mouse embryonic stem cells, its presence at Msp I sites is only approximately one fourteenth that of 5-mC.<sup>17)</sup> A comparison of hydroxymethylation levels, such as methylation levels (5mC+5hmC), between tissues using mouse samples assessed according to the hMSD-AFLP method revealed tissue-specific distribution patterns similar to those of MSD-AFLP method, with levels correlated at many sites (Fig. 3A; see Fig. 4b of Ref. 5) for methylation). Among the sites where methylation levels (5mC + 5hmC) differed between tissues using the MSD-AFLP method, although it cannot be ruled out that some sites may be predominantly 5-hmC, the presence of 5-hmC is approximately 1/14 that of 5-mC. These results suggest that 5-hmC, like 5-mC, may play a role in determining differentiation status and tissue-specific gene expression.

In addition, we found that the rate of change in hydroxymethylation levels was greater in some regions, suggesting that there may be cases in which hydroxymethylated DNA is a more sensitive biomarker. According to previous reports, when comparing methylation and hydroxymethylation in lung tumors and normal tissues, only 1441 sites (2.4%) of the significant different 5hmC overlapped with the significant total

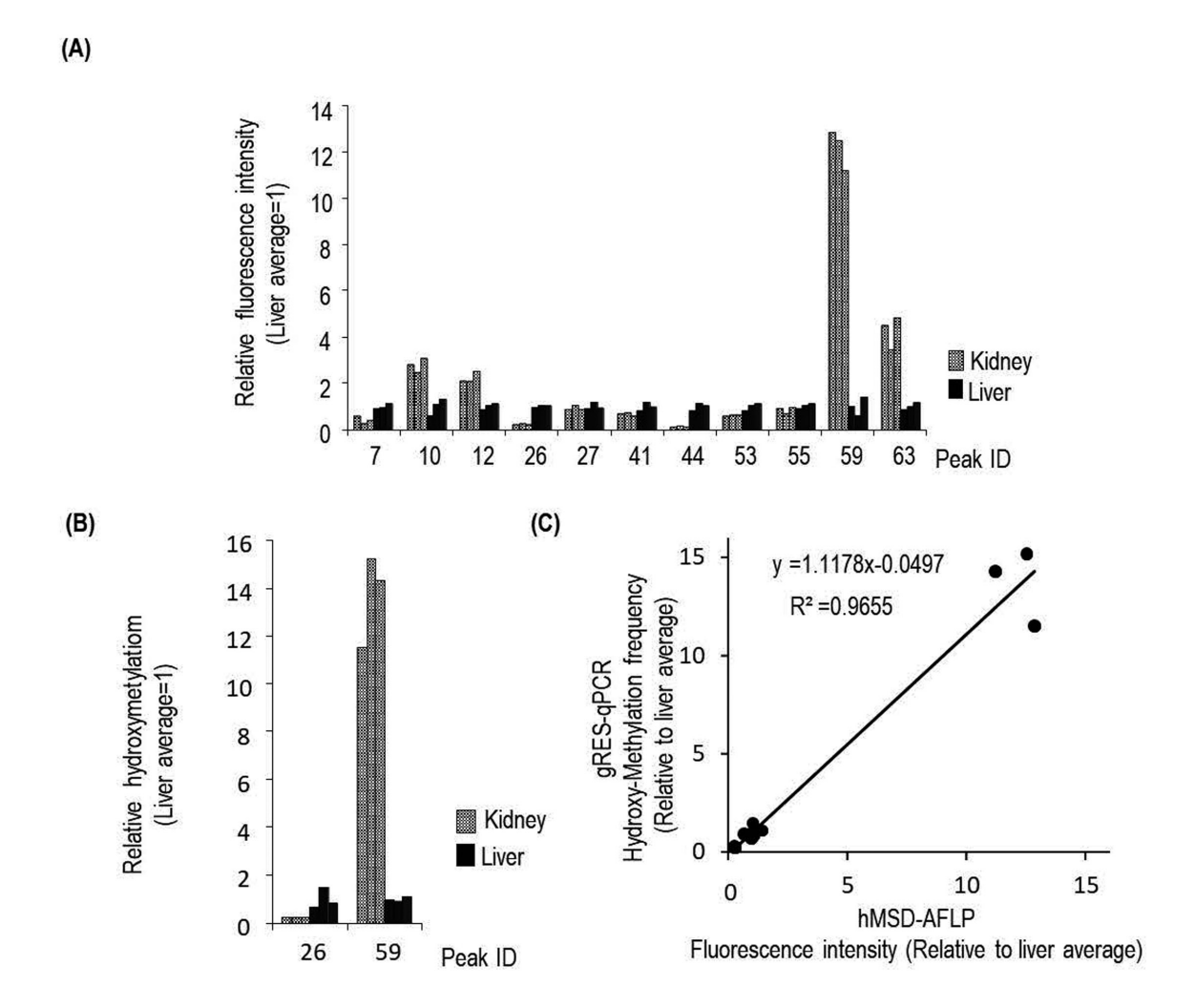


Fig. 3. Confirmation of the Accuracy of hMSD-AFLP Analysis by gRES-qPCR

(A) Relative fluorescence intensity obtained from hMSD-AFLP data. (B) Relative hydroxymethylation levels of 2 CpG sites determined by gRES-qPCR analysis using locus-specific primers. (C) Scatter plot of relative hydroxymethylation level determined using gRES-qPCR analysis and relative fluorescence intensity determined using hMSD-AFLP analysis.

methylation. In addition enrichment analysis suggested that they have different biological functions, raising hopes for 5hmC as a new biomarker. 18) The results of the present study support those of previous studies, suggesting that the present method is able to identify highly sensitive markers for the diagnosis and prognosis of the disease. In this study, we developed an NGS protocol for hMSD libraries in combination with NGS. The reproducibility was evaluated, and R2 was approximately 0.9 regardless of the presence or absence of 6-FAM, indicating sufficient reproducibility. Next, we evaluated this by comparison with AFLP data. Seven of the eight peaks (87.5%) of candidate in AFLP detected as tissue-specific differentially 5hmC, with a good correlation with NGS (R<sup>2</sup> of approximately 0.9). This study used a modified version of the MSD-AFLP method, in which the library structure (internal sequences and lengths of possible fragments) was exactly the same except for the part involving 5GmC or 5mC. Therefore, it is assumed that the protocol for NGS used in this study can also be applied to MSD-AFLP libraries. In the MSD-AFLP method and hMSD-AFLP method, the detection is performed with capillary electrophoresis, which inherently limits resolution due to the potential overlap of the fragments derived from distinct genomic regions. In contrast, NGS overcomes this limitation, enabling enhanced genomic coverage of the MSD-AFLP method and hMSD-AFLP method through the strategic selection and combination of restriction enzymes. For example, replacing the 8-base recognition enzyme Sbf I with the 4-base cutter Mse I allows for the theoretical detection of approximately 2.1 million CpG sites (approximately 10% of the CpG sites in the genome) in the mouse and approximately 2.5 million CpG sites (approximately 7.9% of the CpG sites in the genome) in the human, as estimated using the GFDB database. Furthermore, other 4-base recognition restriction enzymes that are insensitive to DNA methylation and hydroxymethylation—such as BfaI, TaqI, and CviQI—are also available for use in this analysis. By increasing the number of restriction enzymes, for example by using these enzymes simultaneously, the genomic coverage can be further enhanced. Our results suggest that by combining NGS, both the hMSD-AFLP and MSD-AFLP methods will help identify more accurately and smoothly variable gene sites, with improved genomic coverage (over fiftyfold), and will lead to faster biomarker discovery using both methods.

5hmC is particularly abundant in the brain, and its chang-

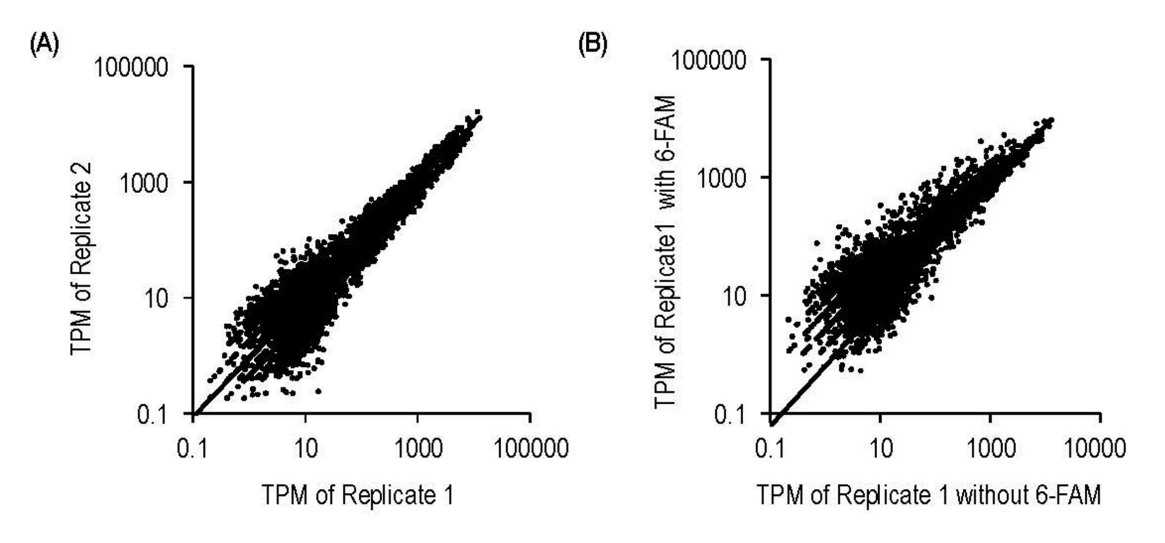


Fig. 4. Reproducibility of NGS

(A) Scatter plot of replicates 1 and 2 without 6-FAM. (B) Scatter plot of replicate 1 without and with 6-FAM.

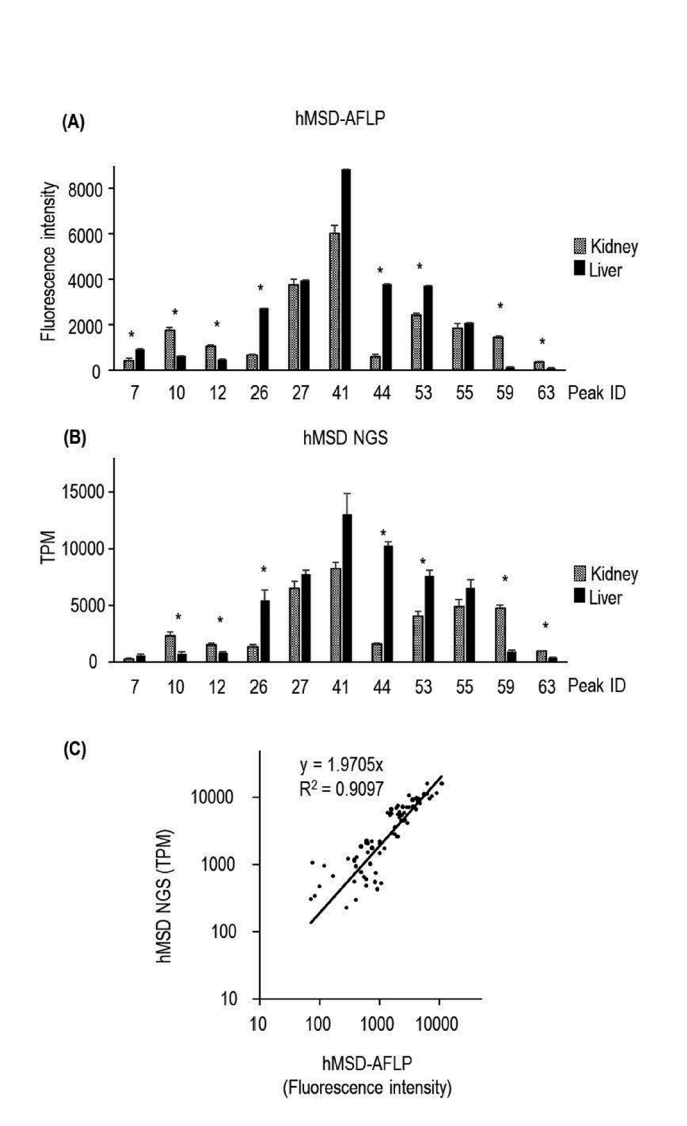


Fig. 5. Confirmation of Consistence Between AFLP and NGS for 11 Fragments

(A) Fluorescence intensity obtained from hMSD-AFLP data. (B) TPM obtained from hMSD NGS data. (C) Scatter plot of hydroxymethylation level determined using AFLP and NGS. \* P < 0.05 by Student's t-test.

es are associated with the neuropathology of Alzheimer's and Parkinson's diseases, making it a promising biomarker and therapeutic target. <sup>19,20)</sup> In addition, 5hmC in cell-free DNA has attracted attention as a promising epigenetic marker for the development, progression, metastasis, and prognosis of various types of cancers, including lung cancer, colorectal cancer, and hepatocellular carcinoma. <sup>21)</sup> This method, along with others, is expected to be applied in the search for biomarkers and therapeutic targets. We conclude that this method, which is based on the MSD-AFLP method, will be useful in various epigenetics-based studies, such as the discovery of biomarkers and therapeutic drug targets, similar to MSD-AFLP.

**Acknowledgment** This work was supported by JSPS KAKENHI Grant Number 21K18091. We would like to thank Editage (www.editage.jp) for English language editing.

**Conflict of interest** The authors declare no conflict of interest.

#### REFERENCES

- De Carvalho DD, You JS, Jones PA. DNA methylation and cellular reprogramming. *Trends Cell Biol.*, 20, 609–617 (2010).
- 2) Feinberg AP. The Key Role of Epigenetics in Human Disease Prevention and Mitigation. *N. Engl. J. Med.*, **378**, 1323–1334 (2018).
- Robles-Matos N, Artis T, Simmons RA, Bartolomei MS. Environmental Exposure to Endocrine Disrupting Chemicals Influences Genomic Imprinting, Growth, and Metabolism. *Genes (Basel)*, 12, 1153 (2021).
- 4) Montano C, Timp W. Evolution of genome-wide methylation profiling technologies. *Genome Res.*, **35**, 572–582 (2025).
- 5) Aiba T, Saito T, Hayashi A, Sato S, Yunokawa H, Maruyama T, Fujibuchi W, Kurita H, Tohyama C, Ohsako S. Methylated site display (MSD)-AFLP, a sensitive and affordable method for analysis of CpG methylation profiles. BMC Mol. Biol., 18, 7 (2017).
- 6) Aiba T, Saito T, Hayashi A, Sato S, Yunokawa H, Maruyama T, Fujibuchi W, Ohsako S. Does the prenatal bisphenol A exposure alter DNA methylation levels in the mouse hippocampus?: an analysis using a high-sensitivity methylome technique. *Genes Environ.*, 40, 12 (2018).
- Aiba T, Saito T, Hayashi A, Sato S, Yunokawa H, Fukami M, Hayashi Y, Mizuno K, Sato Y, Kojima Y, Ohsako S. Exploring disease-specific

- methylated CpGs in human male genital abnormalities by using methylated-site display-amplified fragment length polymorphism (MSD-AFLP). *J. Reprod. Dev.*, **65**, 491–497 (2019).
- Guo JU, Su Y, Zhong C, Ming GL, Song H. Hydroxylation of 5-methylcytosine by TET1 promotes active DNA demethylation in the adult brain. *Cell*, 145, 423–434 (2011).
- Zheng K, Lyu Z, Chen J, Chen G. 5-Hydroxymethylcytosine: Far Beyond the Intermediate of DNA Demethylation. *Int. J. Mol. Sci.*, 25, 11780 (2024).
- 10) Bhattacharyya S, Yu Y, Suzuki M, Campbell N, Mazdo J, Vasanthakumar A, Bhagat TD, Nischal S, Christopeit M, Parekh S, Steidl U, Godley L, Maitra A, Greally JM, Verma A. Genome-wide hydroxymethylation tested using the HELP-GT assay shows redistribution in cancer. *Nucleic Acids Res.*, 41, e157 (2013).
- Thomson JP, Hunter JM, Nestor CE, Dunican DS, Terranova R, Moggs JG, Meehan RR. Comparative analysis of affinity-based 5-hydroxymethylation enrichment techniques. *Nucleic Acids Res.*, 41, e206 (2013).
- 12) He B, Yao H, Yi C. Advances in the joint profiling technologies of 5mC and 5hmC. RSC Chem. Biol., 5, 500-507 (2024).
- Kisil O, Sergeev A, Bacheva A, Zvereva M. Methods for Detection and Mapping of Methylated and Hydroxymethylated Cytosine in DNA. *Biomolecules*, 14, 1346 (2024).
- 14) Sun R, Zhu P. Advances in measuring DNA methylation. Blood Sci., 4, 8–15 (2021).
- 15) Lee SM. Detecting DNA hydroxymethylation: exploring its role in

- genome regulation. BMB Rep., 57, 135-142 (2024).
- 16) Kinney SM, Chin HG, Vaisvila R, Bitinaite J, Zheng Y, Estève PO, Feng S, Stroud H, Jacobsen SE, Pradhan S. Tissue-specific distribution and dynamic changes of 5-hydroxymethylcytosine in mammalian genomes. J. Biol. Chem., 286, 24685–24693 (2011).
- 17) Tahiliani M, Koh KP, Shen Y, Pastor WA, Bandukwala H, Brudno Y, Agarwal S, Iyer LM, Liu DR, Aravind L, Rao A. Conversion of 5-methylcytosine to 5-hydroxymethylcytosine in mammalian DNA by MLL partner TET1. Science, 324, 930–935 (2009).
- 18) Wang Z, Du M, Yuan Q, Guo Y, Hutchinson JN, Su L, Zheng Y, Wang J, Mucci LA, Lin X, Hou L, Christiani DC. Epigenomic analysis of 5-hydroxymethylcytosine (5hmC) reveals novel DNA methylation markers for lung cancers. *Neoplasia*, 22, 154–161 (2020).
- 19) Zhao J, Gu T, Gao C, Miao G, Palma-Gudiel H, Yu L, Yang J, Wang Y, Li Y, Lim J, Li R, Yao B, Wu H, Schneider JA, Seyfried N, Grodstein F, De Jager PL, Jin P, Bennett DA. Brain 5-hydroxymethylcytosine alterations are associated with Alzheimer's disease neuropathology. Nat. Commun., 16, 2842 (2025).
- Min S, Xu Q, Qin L, Li Y, Li Z, Chen C, Wu H, Han J, Zhu X, Jin P, Tang B. Altered hydroxymethylome in the substantia nigra of Parkinson's disease. *Hum. Mol. Genet.*, 31, 3494–3503 (2022).
- Song D, Zhang Z, Zheng J, Zhang W, Cai J. 5-Hydroxymethylcytosine modifications in circulating cell-free DNA: frontiers of cancer detection, monitoring, and prognostic evaluation. *Biomark. Res.*, 13, 39 (2025).